Structure of swirling turbulent flames. Investigation by PIV and spontaneous Raman scattering

Dmitriy K. Sharaborin*[1,2], Dmitriy M. Markovich[1,2], Vladimir M. Dulin[1,2]

[1]Kutateladze Institute of Thermophysics, 1 Ak. Lavrentyeva Avenue, 630090, Novosibirsk, Russia

[2]Novosibirsk State University, 2 Pirogova Street, 630090, Novosibirsk, Russia

*phone: +7-383-3356684, e-mail: sharaborin.d@gmail.com

Abstract: The paper reports on investigation of the spatial structure of turbulent premixed swirling propane/air flames at atmospheric pressure for the equivalence ratio $\Phi = 0.7$ and Reynolds number $Re = 5000$. Distributions of the time-average velocity, density and main species concentration are measured for low- and high-swirl reacting jets. In the latter case, the flow is characterized by a breakdown of the swirling jet's vortex core with the presence of a bubble-type central recirculation zone. For the low-swirl jet the mean axial velocity remains positive. In both cases the flames are stabilized in the inner mixing layer of the jet around the central wake, containing hot combustion products. O_2 and CO_2 concentrations in the wake of the low-swirl jet are found to be approximately two times smaller and greater, respectively, than those in the recirculation zone of the high-swirl jet.

Keywords: swirling flame; low-swirl flame; vortex breakdown; turbulent flame structure; spontaneous Raman scattering; particle image velocimetry

Introduction

Flames in many burners and combustion chambers are stabilized by organizing jet flows with swirl, because it provides successful ignition and stable combustion in a compact zone for a wide range of fuel-to-air ratios [1-3]. In particular, it allows to stabilize flames for fuel-lean conditions, which is an effective technology to reduce NO_x emissions [4]. Optimization of the aerodynamics of combustion chambers is also important, because the oxidation of nitrogen to a sufficient extent takes place in hot combustion products behind the flame front [5]. Likewise, low-swirl flame concept (see [6-8]) has been proved to decrease amount of NOx in the combustion products in comparison to the high-swirl flame at the similar conditions [9]. The improvement is provided by a decrease of the residence time of nitrogen molecules inside the hot zone due to the absence of flow recirculation zone.

A detailed information on the flow structure of turbulent reacting flows can be retrieved by using low-intrusive tracer-based optical techniques such as laser Doppler velocimetry (LDV, [6, 10]) and particle image velocimetry (PIV, [9, 11-13]). PIV provides the spatial velocity distribution for a certain cross-section of the flow. For a more complete description of the processes occurring in the flame, information about the density and temperature distribution is necessary. At the moment there are several methods for measuring the fields of temperature, density and concentration in flames. These methods are based on registration of the local laser-induced fluorescence (LIF), Rayleigh scattering, spontaneous Raman scattering (SRS) and coherent anti-Stokes Raman scattering (CARS) [14-16]. LIF-

based methods are characterized by high intensity of the detected signal, but the quantitative interpretation of the data is difficult, and sometimes impossible at all, due to the unknown quenching rate of the fluorescence. The planar registration of Rayleigh scattering allows estimating the local density in the flow cross section, but requires a priori information about the resulting scattering cross section of molecules at each measurement point. Interpretation of SRS signal during vibrational transitions of a specific type of molecule at temperature measurements does not require *a priori* information of the concentration of other molecules and provides information on the relative concentration of the main components of the gas mixture. SRS measurements can be also performed for 1D (along the beam) and 2D (in plane) configurations [17, 18]

The main aim of the present work is to compare time-averaged spatial structure of low- and high-swirl turbulent premixed lean flames by using the PIV and SRS techniques. Swirl effect on the local velocity, density and mean species concentration distributions is the main focus of the present study.

Experimental setup

Sketch of the experimental setup for 2D measurements is shown in fig. 1. The measurements were carried out using a combustion rig consisted of a swirl burner, flow seeding device, premixing pipe and section for the air and propane flow rate control. The burner was a contraction nozzle (with the exit diameter d = 15 mm) with vane swirler inside. A swirl rate of the flow (the ratio between the angular and axial jet momentum fluxes) was varied by using swirlers with different inclination angles of the blades. The swirl rates were estimated based on the geometric parameters of the swirlers [1]:

$$S = \frac{2}{3}\left(\frac{1-\left(d_1/d_2\right)^3}{1-\left(d_1/d_2\right)^2}\right)\tan\left(\psi\right) \quad (1)$$

Here d_1 = 7 mm is the diameter of the centerbody supporting the vanes, d_2 = 27 mm is the external diameter of the swirler, and ψ is the vanes inclination angle relatively to the axis. Swirlers with ψ = 30°and 55° were used provide the swirl rates of S = 0.41 and 1.0, respectively. The Reynolds number Re_{air} (based on d, the bulk velocity of the air flow at the nozzle exit U_0 = 5 m/s, and viscosity of the air) was 5 000. The equivalence ratio Φ of the propane-air mixture was 0.7. In order to provide the PIV measurements, the flows were seeded by TiO_2 particles (with the average size of 1 μm). The mass fraction of the particles in the jet was less than 0.03%. The seeding device introduced solid particles to the air flow by using a stirring rod.

The PIV system was composed of a double-pulsed Nd:YLF Pegasus PIV laser and a pair of PCO 1200HS CMOS cameras. System was running at approximately 770 Hz repetition frequency. The PIV laser sheet, formed by a system of cylindrical and spherical lenses, passed thru the central plane of the flows and had a thickness of 0.8 mm in the measurement region. The cameras were equipped with narrow-bandwidth optical filters admitting the light from the laser and suppressing the radiation of the flame. The system was operated by a computer with in-house "ActualFlow" software. Stereo calibration was performed using a multi-level calibration target and 3rd-order polynomial transform. For each flow case, 2400 instantaneous three-component velocity fields were measured via three independent runs. The data processing was similar to that in the previous stereo PIV investigation of the swirling flames [19]. The error analysis of the PIV measurements in the reacting flows due to finite spatial and temporal resolution, including those caused by the particle inertia, was reported by [13].

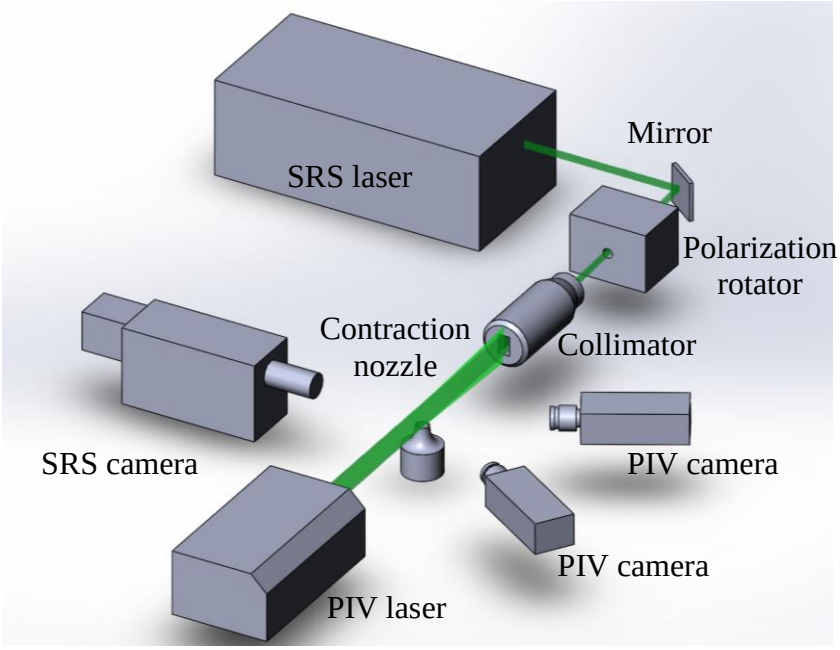

Figure 1. Sketch of the experimental setup for 2D SRS and stereo PIV measurements

The third (355 nm) or the second (532 nm) harmonic of a pulsed Quanta-Ray Nd:YAG laser was used for the illumination during SRS measurements. The energy of 6 ns laser pulses was monitored by a Coherent LabMax-TOP energy meter. The pulse energy of 355 and 532 nm beams was 200 and 690 mJ, respectively, with 5% RMS fluctuations. During 1D measurements the laser beam was focused with the spot diameter less than 0.8 mm. A collimating optics was used to produce the laser sheet for 2D measurements with the width of 45 mm and thickness less than 0.8 mm in the measuring area. The SRS signal was registered by a 16-bit ICCD camera (Princeton instruments PI-MAX-4 with GEN II type of the photocathode). During 1D spectroscopy the scattered light was captured by a Czerny-Turner spectrograph (Newport MS127i 1/8 m), equipped with a UV lens. In the case of 2D SRS spectroscopy, the camera was equipped with a band-pass tunable Lyot optical filter (VariSpec LC), based on liquid crystals. 2D intensity of the Stokes component of the 2D SRS by nitrogen molecules (vibrational-rotational transitions) was recorded in the wavelength range 607.3 ± 5 nm. An additional multi-notch holographic filter was used to block radiation of the Rayleigh scattering, which was not completely blocked by the tuneable filter.

To improved signal-to-noise ratio, each frame captured by the camera was accumulated from SRS signal of 250 laser pulses and was also processed by 8×8 pixels binning. Fifty images were captured and averaged for each measured flame regime to suppress read-out noise of CCD. For further increase of the signal-to-

noise ratio, the SRS signal was recorded for two perpendicular linear polarizations of the laser radiation by using a half-wave plate. Signal for the polarization parallel to the scattering plane was subtracted from that for the perpendicular polarization to minimize contribution of the background light, fluorescence and dark current of the photocathode to the SRS data.

Figure 2 shows example of 1D SRS signal across the swirling jet with combustion. There are four different zones. The surrounding air is for $x/d > 0.75$. The annular fuel-air jet surrounds the flame front (a thin layer with remaining broadband fluorescence at approximately 0.5 of x/d) and mixing with the atmospheric air. The reaction zone surrounds central wake region, containing hot combustion products with temperature above 1800 K, where the signal-to-noise ratio is evaluated as 1:9 and 1:1.7 for the Stokes and anti-Stokes components of the SRS for rotational-vibrational transitions of the N_2. Intensity of the anti-Stokes components of the SRS in the ambient air and reacting flow did not exceed 2% of the Stokes SRS intensity in the air. It was not accounted for during density evaluation because the population of the first vibrational energy level did not exceed 15% for the temperatures below 1800 K.

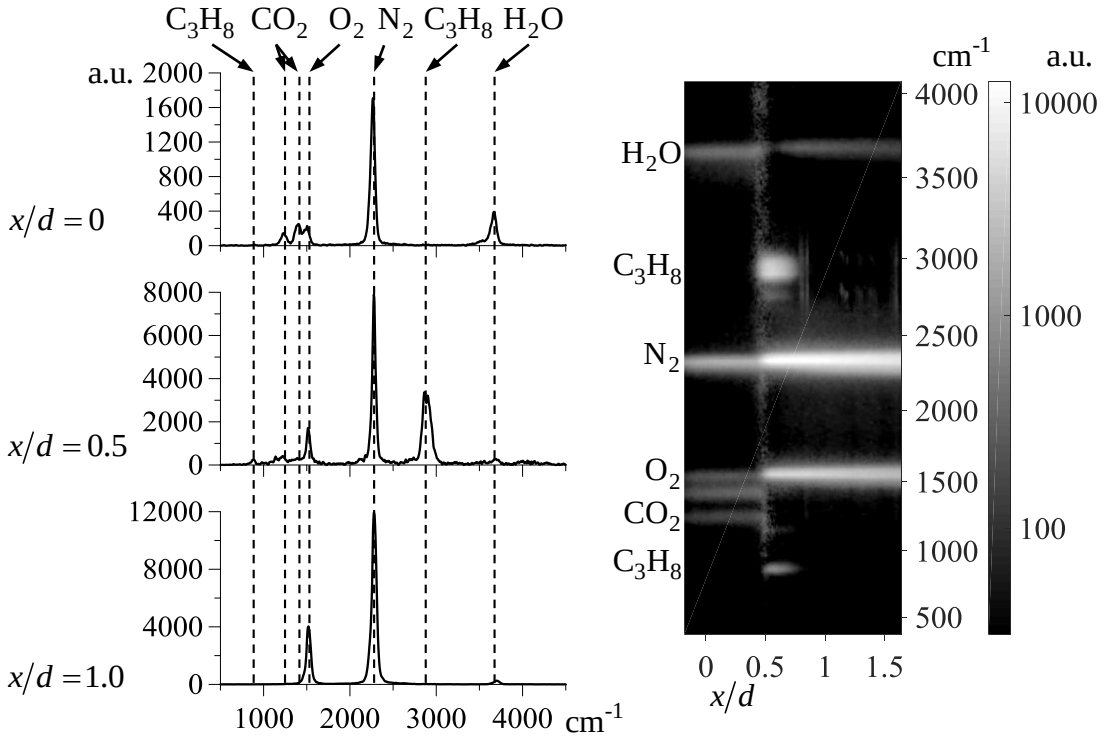

Figure 2 Example of Stokes SRS spectra along laser beam intersecting a turbulent high-swirl (S = 1.0) propane/air flame at height of $y = 0.5d$ downstream the nozzle exit

The data processing for the 1D measurements is similar to that performed by [17]. 2D data processing is based on the ratio between the Stokes components of the rotational-vibrational transitions of the nitrogen in the reacting jet and atmospheric air (when the jet flow was switched off). A more detailed description of the signal processing is given in [20].

Results

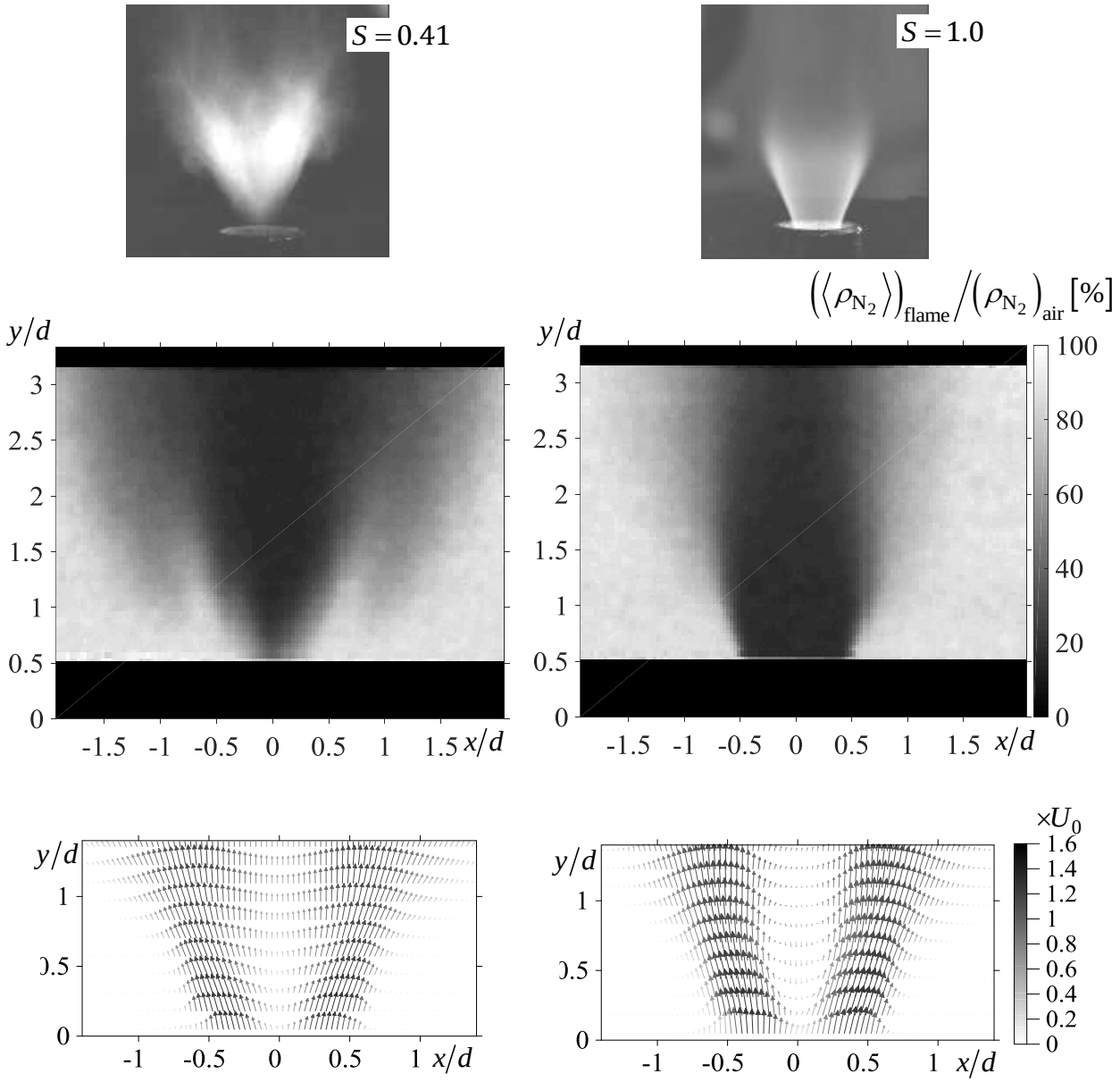

Figure 3 Photographs of the flames and distributions of the mean normalized density and velocity in low-swirl (S = 0.41) and high-swirl (S = 1.0) lean propane/air lean flames

Figure 3 shows the photographs and distributions of the mean velocity and local density of the nitrogen in the low- and high-swirl lean propane/air flames. For both swirl intensities, there are wake regions present at the jet axis, where the local gas density is approximately 6 times lower than that in the surrounding air. For the low-swirl flow the axial velocity reaches minimum near $y/d = 0.5$ but remains

positive, indicating that there is no recirculation zone. The flame front stabilizes around this region. For the high-swirl rate there is a central recirculation zone, partially present in the nozzle. The flame front surrounds it and also penetrates into the nozzle. According to the photographs, the flame for the high-swirl flow is less turbulent. This could be due to suppression of turbulent fluctuations by the combustion inside the nozzle.

Figure 4 shows the distributions of the temperature and main gas species concentrations for three cross-sections of the reacting jets. There was no sufficient concentration of CO detected in the spectra (see Figure 2). The molar fraction of N_2 is 76±2% for the entire cross-section, indicating that it is a good passive tracer (since it is almost not consumed during the chemical reactions) for 2D SRS measurements of the local gas density. For y/d = 0.5 and y/d = 1.5 cross-sections of the high-swirl case, the fuel/air jet surrounds the recirculation zone containing the combustion products with 11% of H_2O, and 7±1% of CO_2 and O_2. The temperature inside the recirculation zone reaches 1845 K. For the low-swirl flame the hot combustion products also tend to concentrate inside the wake. Remarkable, that for the y/d = 1.5 and y/d = 2.5 cross-sections the O_2 concentration has minimum of approximately 3% at the axis of the low-swirl jet. CO_2 concentration in the wake is almost two times greater than that for the high-swirl jet. Moreover, the temperature at the axis of the low-swirl jet almost reaches 2000 K for y/d =1.5, whereas the adiabatic flame temperature for a propane/air mixture at normal temperature and

pressure is 1875 K. This effect of the low swirl on stratification of the combustion products deserves additional study.

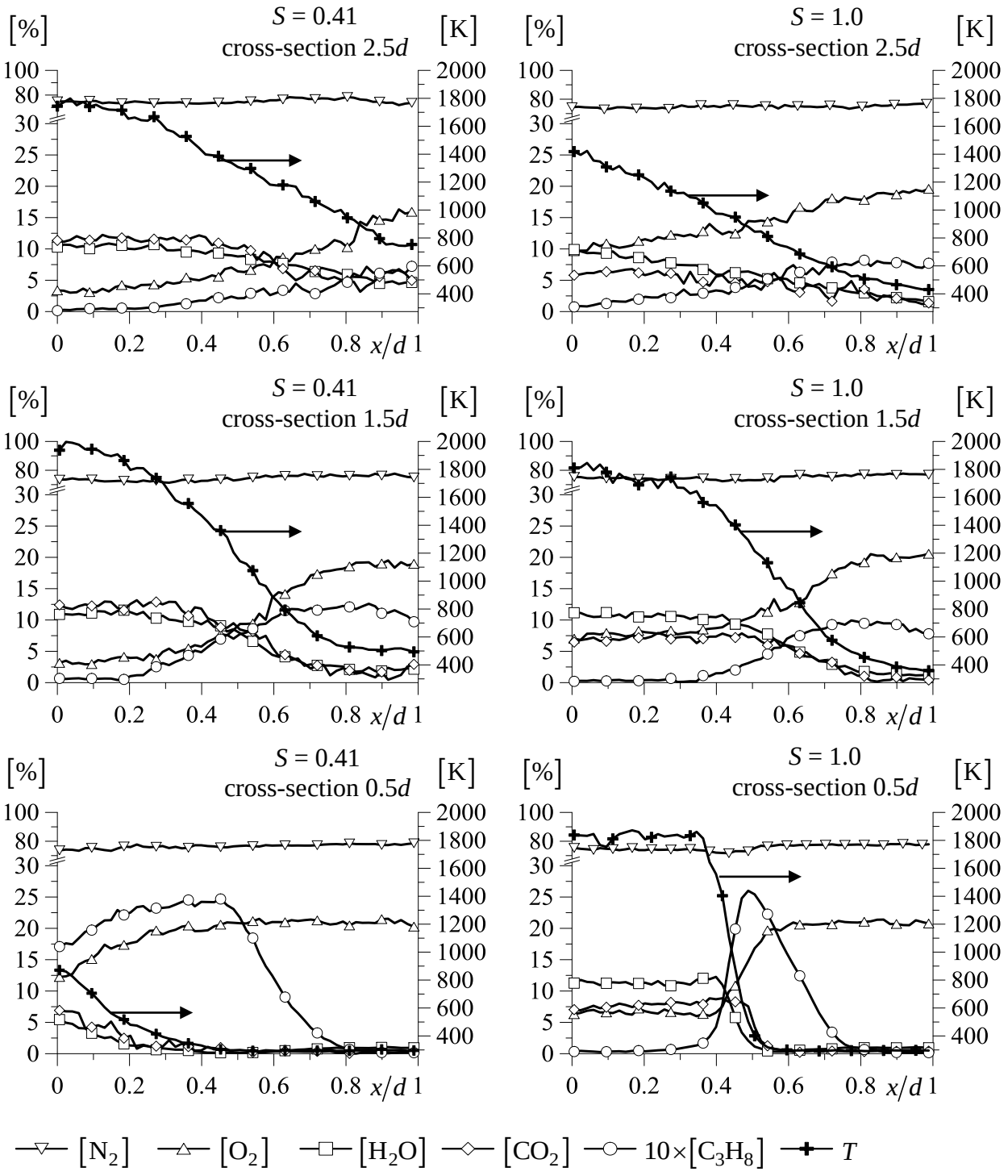

Figure 4 Distributions of the mean temperature and main species concentration in low-swirl (S = 0.41) and high-swirl (S = 1.0) lean propane/air flames (Φ = 0.7)

Conclusion

A comparative study of the time-averaged flow and flame structure of turbulent premixed propane/air lean flames has been performed by using the PIV and SRS techniques. In both cases the swirling jet flows, issuing from the burner, were featured by the presence of a wake zone at the jet axis. The flame stabilized in the inner mixing layer between the wake and the annular fuel/air jet flow used from the nozzle. For the high-swirl case there is a recirculation of the hot combustion products with remaining oxygen. For the low-swirl jet the oxygen concentration carbon dioxide in the wake are found to be twice lower and higher, respectively, than those in the recirculation zone of the high-swirl jet.

Acknowledgments

This research is funded by Russian Science Foundation (grant № 16-19-10566). Continuous support and fruitful discussions by Prof. Kemal Hanjalić are kindly acknowledged.

References

1. **Gupta, A. K., D. G. Lilley, N. Syred.** Swirl flows. Kent, U.K.: Abacus Press. 1984.
2. **Syred N., Beer J. M.** Combustion in swirling flows: a review //Combust. Flame. – 1974. – V. 23. – P. 143-201.
3. **Weber R., Dugué J.** Combustion accelerated swirling flows in high confinements //Progr. Energy Combusti. Sci. – 1992. – V. 18. – P. 349-367.
4. **Dunn-Rankin D.** Lean combustion: Technology and control. Academic Press, Elsevier. 2008.
5. **Zel'dovich, Ya. B., P. Ya. Sadovnikov, D. A. Frank-Kamenetskiy.** Okislenie azota pri gorenii [Oxidation of nitrogen during combustion]. Moscow–Leningrad: Izd-vo AN SSSR. 1947.
6. **Cheng R.K.** Velocity and scalar characteristics of premixed turbulent flames stabilized by weak swirl //Combust. Flame. – 1995. – Vol. 101. – P. 1-14
7. **Yegian D.T., Cheng R.K.** Development of a lean premixed low-swirl burner for low NOx practical applications //Combust. Sci. Technol. – 1998. – Vol. 139. – P. 207-227.
8. **Cheng R.K.** Low swirl combustion // In: The Gas Turbine Handbook (Ed.: Dennis R.) Department of Energy, Washington, DC. 2006. P. 241–255.
9. **Johnson M.R., Littlejohn D., Nazeer W.A., Smith K.O., Cheng, R.K.** A comparison of the flowfields and emissions of high-swirl injectors and low-swirl injectors for lean premixed gas turbines //Proc. Combust. Inst. – 2005. – Vol. 30. – P. 2867-2874.
10. **Edwards C.F., Fornaciari N.R., Dunsky C.M., Marx K.D., Ashurst W.T**. Spatial structure of a confined swirling flow using planar elastic scatter imaging and laser Doppler velocimetry //Fuel. – 1993. – Vol. 72. – P. 1151-1159.
11. **Stella A., Guj G., Kompenhans J., Raffel M., Richard H.** Application of particle image velocimetry to combusting flows: design considerations and uncertainty assessment // Exp. Fluids. – 2001. – Vol. 30. – P. 167-180.
12. **Cheng R.K., Littlejohn D., Nazeer W.A., Smith K.** Laboratory studies of the flow field characteristics of low-swirl injectors for adaptation to fuel-flexible turbines //J. Eng. Gas Turbines Power. – 2008. – Vol. 130. – 021501
13. **Korobeinichev O.P., Shmakov A.G., Chernov A.A., Markovich D.M., Dulin V.M., Sharaborin D.K.** Spatial and temporal resolution of the particle image velocimetry technique in flame speed measurements // Combust. Expl. Shock Waves. – 2014. – V. 50. – P. 13-21.
14. **Kohse-Höinghaus K.** Laser techniques for the quantitative detection of reactive intermediates in combustion systems //Progr. Energy Combust. Sci. –1994. – Vol. 20. – P. 203-279.
15. **Hassel E. P., Linow S.** Laser diagnostics for studies of turbulent combustion //Meas. Sci. Technol. – 2000. – V. 11. – P. R37-R57.

16. **Miles R.B., Lempert W.R., Forkey J.N.** Laser Rayleigh scattering //Meas. Sci. Technol. – 2001. – Vol. 12. – P. R33-R51
17. **Rabenstein F., Leipertz A.** One-dimensional, time-resolved Raman measurements in a sooting flame made with 355-nm excitation. // Appl. Optics. – 1998. – Vol. 37. – P. 4937-4943.
18. **Schefer R.W.** Three-dimensional structure of lifted, turbulent-jet flames //Combust. Sci. Technology. – 1997. – Vol. 125. – P. 371-394.
19. **Alekseenko S.V., Dulin V.M., Kozorezov Y.S., Markovich D.M., Shtork S.I., Tokarev M.P.** Flow structure of swirling turbulent propane flames //Flow Turb. Combust. – 2011. – V. 87. – P. 569-595/
20. **Sharaborin D.K., Dulin V.M., Lobasov A.S., Markovich D.M.** Measurements of density field in a swirling flame by 2D spontaneous Raman scattering //AIP Conf. Proc. - 2016. - V. 1770. - P. 030027.